ADVANCED MATERIALS
www.advmat.de

Engineering Biomolecular Self-Assembly at Solid–Liquid Interfaces

Shuai Zhang, Jiajun Chen, Jianli Liu, Harley Pyles, David Baker, Chun-Long Chen, and James J. De Yoreo*

Biomolecular self-assembly is a key process used by life to build functional materials from the "bottom up." In the last few decades, bioengineering and bionanotechnology have borrowed this strategy to design and synthesize numerous biomolecular and hybrid materials with diverse architectures and properties. However, engineering biomolecular self-assembly at solid–liquid interfaces into predesigned architectures lags the progress made in bulk solution both in practice and theory. Here, recent achievements in programming self-assembly of peptides, proteins, and peptoids at solid–liquid interfaces are summarized and corresponding applications are described. Recent advances in the physical understandings of self-assembly pathways obtained using in situ atomic force microscopy are also discussed. These advances will lead to novel strategies for designing biomaterials organized at and interfaced with inorganic surfaces.

Dr. S. Zhang, Dr. J. Chen, Dr. J. J. De Yoreo
Department of Materials Science and Engineering
University of Washington
Seattle, WA 98105, USA
E-mail: zhangs71@uw.edu

Dr. S. Zhang, Dr. J. Chen, Dr. J. Liu, Prof. C.-L. Chen, Dr. J. J. De Yoreo
Physical Sciences Division
Physical and Computational Sciences Directorate
Pacific Northwest National Laboratory
Richland, WA 99352, USA

Dr. J. Liu
School of Materials Science and Engineering
Dongguan University of Technology
Dongguan, Guangdong 523830, China

Dr. H. Pyles, Prof. D. Baker
Department of Biochemistry
University of Washington
Seattle, WA 98195, USA

Dr. H. Pyles, Prof. D. Baker
Institute for Protein Design
University of Washington
Seattle, WA 98195, USA

Prof. D. Baker
Howard Hughes Medical Institute
University of Washington
Seattle, WA 98195, USA

Prof. C.-L. Chen
Department of Chemical Engineering
University of Washington
Seattle, WA 98195, USA

The ORCID identification number(s) for the author(s) of this article can be found under https://doi.org/10.1002/adma.201905784.

DOI: 10.1002/adma.201905784

1. Introduction

Self-assembly is an efficient bottom-up process to organize matter across length scales. In nature, the outstanding precision, efficiency, and adaptability of biomolecular self-assembly are responsible for the emergence, evolution, and continuation of life.[1,2] The molecular building blocks, mainly peptides, proteins, and nucleic acids, spontaneously assemble into hierarchical structures and complexes. For example, ion channels, DNA duplexes, actin filaments, and collagen fibrils are encoded with high information content enabling them to then integrate into larger structures (e.g., mitochondria, nucleosomes, muscles, and bones) and thus fulfill a wide variety of functions, including energy conversion, storage and transportation of matter and information, force generation, and mechanical support.[3,4]

In the last two decades, researchers in bioengineering and bionanotechnology have been inspired by nature's dramatic ability to design and fabricate bionanomaterials with emergent properties from the "bottom up."[4,5] One successful example is DNA nanotechnology, in which Watson–Crick base-pairing rules are used to manipulate DNA into complex architectures with broad diversity and applications in diagnosis, drug delivery, sensing, imaging, and computing.[6,7] Another successful example is peptide self-assembly, which has been inspired by formation of amyloid fibrils driven by beta-strand pairing; this strategy has been adopted to design peptide-based hybrid materials via hydrogen bonding and side-chain interactions, with applications in biomedical engineering, tissue engineering, electronic nanodevices, biomimetics, and biosensors.[8,9]

Protein assembly represents a third, rapidly growing field. Structural complexity, heterogeneity, accuracy, and diversity make proteins versatile building blocks for novel supramolecular nanomaterials with high order and a broad range of functions.[3,10] Using various self-assembly strategies, such as fusion of symmetric interfaces, de novo design of noncovalent protein–protein interfaces, and insertion of reversible metal-ion coordination and/or disulfide bonds, well-ordered protein architectures with many point group symmetries in 1D, 2D, and 3D have been achieved.[3,11–13] These materials have a wide range of potential applications in biocatalysis, biomineralization, nanofabrication, drug design and delivery, and diagnosis.

The fourth group of self-assembling building blocks that have gained recent interest are sequence defined biomimetic molecules, such as peptoids, which are a class of sequence-defined synthetic foldamers, developed to mimic both the structure and function of peptides and proteins, bridging the gap between biopolymers and synthetic polymers.[14] Various amphiphilic peptoids that self-assemble into biomimetic nanomaterials with hierarchical structures, both on substrate surfaces and in solution, have been designed recently.[15–22]

With the exception of DNA, which assembles following simple base-pairing rules, previous studies have revealed that biomolecular self-assembly is mainly driven by a complex balance of noncovalent interactions including hydrogen bonds, hydrophobic interactions, electrostatic interactions, and π–π interactions. However, external conditions, such as pH, temperature, and ionic strength, also play essential roles in controlling assembly.[23] The design, formation, properties, and applications of various biomolecular assembly systems have been comprehensively summarized and discussed in recent reviews.[24–26]

In contrast to the extensive progress made in engineering biomolecular self-assembly in bulk solutions, progress at solid–liquid interfaces has lagged behind. Even though interactions between biomolecules and inorganic surfaces are known to be essential to many biological functions, including the growth of bone within collagen matrixes and the promotion and inhibition of ice crystallization by ice-binding proteins,[27] the detailed structure and dynamics of most biomolecular–inorganic interfaces are not clear.[28]

Although observations of self-assembly on inorganic surfaces by numerous biomolecules, including artificially designed peptides,[29,30] collagen,[31] streptavidin,[32] S-layer proteins,[33,34] and glucose,[35] have been reported and a general discussion of what is known about the influence of substrates on biomolecular self-assembly was presented in a recent review,[25] detailed physical models that can quantitatively explain such observations are lacking. The recent development of multimodal and high-speed atomic force microscopy (AFM) techniques has helped in this regard by providing a capability to study complex biological systems.[36,37] In particular, these developments have enabled in situ monitoring of biomolecular self-assembly processes on surfaces with submolecular spatial resolution and (sub-)second temporal resolution, which is typically adequate to simultaneously capture detailed structures and assembly pathways. However, in none of the cases cited above have the biomolecular interfaces been predesigned to match the solid surfaces and thereby direct assembly. Hence the structure and degree order resulting from self-assembly at interfaces has been hard to manipulate[38] and control of higher-level order remains challenging.

Herein, we review some recent achievements in the engineering of peptide, protein, and peptoid self-assembly at solid–liquid interfaces. We explicitly discuss programming of interfaces between the building blocks and the lattice of solid surfaces in a predefined manner. We also describe recently developed models and principles elucidated via in situ AFM studies of self-assembly of these systems at solid–liquid interfaces. Remaining knowledge gaps and practical and theoretical challenges are discussed as well.

2. Peptides

As a simplified model system for proteins, (oligo)peptides are widely used to study the interactions between proteins and inorganic surfaces. Due to the development of the phage display technique, various peptides can be screened and selected for their strong and specific binding affinity to a wide range of inorganic surfaces and can subsequently be utilized to control the morphological outcome and phases of these inorganic materials.[39–44] For example, Chiu et al. used selected peptides to tune the size of Pt nanoparticles by controlling their nucleation and growth kinetics.[43] Moreover, geometries of these Pt nanoparticles could be controlled using facet-specific peptides as regulating agents[44] (**Figure 1**a,b). In a recent study, Zhu et al. showed that these peptides could further drive the self-assembly of Pt nanocubes into large-area, long-range, [100] linear structures.[42] Together, these works open vast opportunities for multiscale programmable structures of inorganic nanoparticles.

In some cases, these selected peptides not only adsorb onto the target surfaces; they also assemble into highly ordered structures.[45–47] Such assembled peptide layers can modify the surface chemistry or physical properties of the substrate, providing opportunities for various applications, such as 2D materials synthesis, biosensing, bioelectronic devices, and implantable medical devices.[8,45,47,48] For example, Hayamizu et al. selected peptides that assembled into nanowires on 2D materials such as graphene and MoS_2 and modified both the electrical conductivity and the photoluminescence of the underlying 2D substrates.[48] In another example, relying on nanomechanical symmetry breaking effects under AFM tip scanning, Hong et al. reported the successful construction of an in-plane, unidirectional molecular array on graphene.[49] Assembled domains were aligned along a selected symmetry axis of the graphene lattice under finely tuned scanning conditions after removing previously adsorbed domains. The local symmetry breaking of the directional equivalence of the surface, which leads to unidirectional 1D assemblies, opens new possibilities to precisely control assembly of engineered peptides at solid interfaces. This control may be a crucial step toward integrating biology with nanoelectronics in fully self-assembled bio-nanoelectronic devices.[48]

Using a series of graphite binding peptides and mutants, researchers have systematically studied their assembled structures, stabilities, and relationships between peptide sequence and final architectures, as well as influences from other factors, including thermal stimuli, electrochemical controls, and surface charge.[8,23,45,47,48] However, the pathways and detailed mechanisms of assembly were not clear, as in situ recording and analysis of the self-assembly processes was limited. Whether self-assembly followed a direct nucleation pathway, which is described by concepts of classical nucleation theory or fell within the broader context of so-called "nonclassical" pathways involving formation, aggregation, and transformation of transient precursors[50] remained unknown.

In a recent study, Chen et al. developed a detailed understanding of the nucleation pathway during assembly of a phage-display selected peptide on MoS_2 surfaces.[51] In this work, a

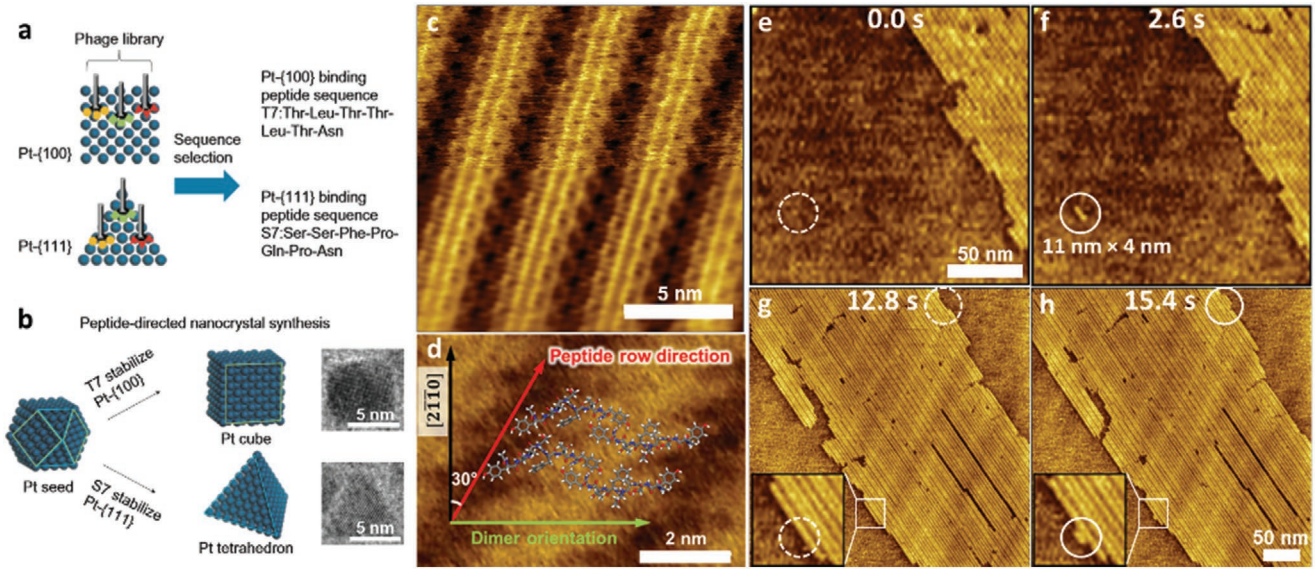

Figure 1. Morphological control of Pt nanocrystals using peptides selected by phage display and row-by-row growth process of 2D peptide films on MoS_2 surfaces. a,b) Schematic illustration of facet-specific peptide selection and nanocrystal synthesis: Pt nanocubes and nanotetrahedrons were obtained from reactions regulated by T7 and S7 peptides, respectively. c) High-resolution image showing detailed row structure in the assembled peptide array. The bottom half of C was FFT filtered. d) Overlapping of the most stable dimer conformation from MD simulations on an AFM image. e–h) In situ high-speed AFM images showing the nucleation of a single row and creation of new rows adjacent to existing ones. a,b) Reproduced with permission.[44] Copyright 2011, Springer Nature. c–h) Reproduced with permission.[51] Copyright 2018, The Authors, published by American Association for the Advancement of Science.

short peptide with specific binding affinity to MoS_2 (001) was used to investigate the assembly of 2D peptide arrays by monitoring their nucleation and growth with in situ AFM and simulating the structural relationships using molecular dynamics (MD). Molecular resolution images provided detailed structural information (Figure 1c) and defined the epitaxial relationship between the peptides and the substrate. Combining the imaging with the MD simulations allowed critical peptide–substrate interactions and the conformations of peptides in the arrays to be determined (Figure 1d). Moreover, molecular-resolution imaging and high-speed movies revealed that peptide assembly followed a direct nucleation pathway (Figure 1e–h), with the initial peptide clusters exhibiting the same order as the final 2D arrays. A model based on a set of rate equations for peptide attachment and detachment was also developed to fully understand the kinetics of nucleation and growth of the assemblies.

The results also revealed the impact of dimensionality on nucleation. In situ AFM revealed a row-by-row growth mechanism of the 2D arrays. New peptide rows were observed as they formed and were found to grow at the same speed regardless of their sizes. In addition, new rows appeared as soon as the peptide concentration exceeded the solubility limit of the 2D arrays, and their rates of nucleation scaled linearly with peptide concentration. These phenomena would only be expected if there was no free energy barrier to nucleation. The findings provided direct molecular-level evidence for a longstanding but unproven prediction of classical nucleation theory for 1D crystals.

Substituting graphite for MoS_2 revealed another assembly pathway made possible through the row-by-row growth process. The peptides still assembled into similar 2D films, but most of the rows comprising these films began as isolated independent nuclei. Over time, these peptide rows, which were immobile on MoS_2, were able to diffuse across the graphite surface and aggregate to form the final compact, highly ordered 2D domains. These results highlight the key roles of epitaxial matching and peptide-surface interaction in tuning assembly pathways.

The peptides investigated in this work exhibit structural features common to many polymeric and chain-like organic molecules that self-assemble on surfaces.[52,53] They may also follow a similar mechanism. The above findings place these systems in the context of well-developed theories for the emergence of order and postnucleation growth and provide a guide for interpreting and controlling their assembly. The understanding gained about the dominant pathways and key parameters that control both pathway selection and growth kinetics should enable researchers to precisely control the morphologies and phases of the assembled structures.

3. Proteins

Proteins are polypeptide chains that fold into complex 3D structures via intramolecular noncovalent interactions. Compared to peptides, protein building blocks are much larger. Although protein molecules are frequently monodispersed, they are far more complicated and anisotropic in their geometry, local charge, and hydrophobicity. In nature, the balance between covalent bonds and noncovalent interactions are tuned to create proteins with specific architectures and functions.[3,54]

In recent years, protein-based 2D assemblies have attracted attention, as many functional 2D protein crystals, such as

bacterial S-layer protein/crystal[33,34] and purple-membrane assemblies,[55] have been found in nature. In the field of protein engineering, researchers have fabricated 2D free-standing protein architectures by manipulating distinct chemical interactions between protein building blocks[11,56] and have designed de novo protein structures.[57] However, there are few reports about building 2D protein crystals at solid–liquid interfaces.[29,32,35,58,59] The involvement of solid–liquid interfaces makes the case far more complicated. The charge and hydration layer near inorganic surfaces have proven to be dramatically different from that of the bulk solution,[60,61] and thus can modulate the noncovalent inter-protein interactions. Additionally, the design of protein interfaces to predictively control self-assembly on inorganic surfaces is rarely undertaken. Given that protein assembly on solid–liquid interfaces is a long-known phenomenon, and it has promising potential in biocompatible devices and protein-mineral composites, improving the capabilities to artificially engineer protein self-assembly at solid interfaces and sharpening the corresponding fundamental knowledge are necessary.

Recently, Pyles et al. reported attempts to control protein assembly on mica (001) through designed protein interfaces and tuning protein–protein noncovalent interactions via electrolytes (**Figure 2**).[62] The work not only proved the capability of de novo design to program protein-inorganic interactions with accuracy at the nanoscale, but also improved the understanding of protein dynamics at solid–liquid interfaces. In this work, the authors mutated the de novo designed helical repeat protein (DHR10) to contain carboxylate residues which geometrically match the K^+ sublattice of the mica (001) plane. The new protein, DHR10-mica*X* (*X* = the number of repeat subunits per molecule), was expected to bind on mica surfaces along the three close-packed directions of the K^+ sublattice (Figure 2a,b).

AFM studies showed that the coverage and packing order of DHR10-mica18 on muscovite mica (*m*-mica) increased if the concentration of KCl was increased (Figure 2c,d). In 10×10^{-3} M KCl, DHR10-mica18 molecules adsorbed on the surface, but were isolated from one another. When [KCl] was increased, DHR10-mica18 was more mobile on the surface and began to form coaligned domains and self-assembled into 2D liquid-crystal phases. These results suggest that electrostatic screening favored protein–protein interactions. Surprisingly, at very high [KCl], DH10-mica18 self-assembled into a 2D smectic liquid-crystal phase with one dominant orientation (Figure 2d) across several-millimeter-square areas. This phase of the protein nanorods likely arises from the increase in translational entropy due to the alignment of the protein nanorods at high volume fraction[63] combined with the (previously reported) twofold anisotropy in the distribution of hydroxyl groups in the underlying *m*-mica (001),[32,35] which breaks the threefold symmetry associated with the aluminosilicate lattice.

To further verify that this hypothesis of entropy-driven colloidal self-assembly of the nanorods was valid to explain the behavior of DHR10-mica18 on the *m*-mica surface, the authors checked the self-assembly of DHR10-mica6, which has a smaller aspect ratio. In 3 M KCl, DHR10-mica6 remained in a 2D liquid phase, indicating the translational entropy gain was not enough to compensate for the conformational entropy lost through condensation into a 2D liquid-crystal phase. This finding agrees with the predictions of theories based on entropy-driven condensation in three dimensions. However, once weak hydrophobic interactions between the ends of protein nanorods were introduced, shorter protein nanorods, like DHR10-mica6-NC and DHR10-mica2-NC, were able to assemble into long, coaligned nanowires. The long-range order of the nanowire matrix again reflected the twofold anisotropy of the underlying *m*-mica (001) (Figure 2f). The long-range order was broken if the substrate was changed to fluorophlogopite mica (f-mica) (Figure 2g).

Finally, short DHR10-mica*X* (*X* = 3, 4, 5, 6, 7) monomers were assembled with a designed trimer interface. The new protein molecules DHR10-mica*X*-H formed open hexagonal networks (Figure 2h–j) in 3 M KCl. The dimension of the hexagonal lattice was digitally determined by the number of repeat units in each monomer. Originally these molecules were predicted to form a close-packed layer; the unexpected open pattern that was observed is again presumed to be the outcome of the balance between protein-mica binding affinity and noncovalent—mainly—entropic, protein–protein interactions.

In summary, this work, on the one hand, proves the feasibility of programming protein interfaces to engineer the final self-assembly at a solid–liquid interface; but, on the other hand, it reminds us that weak protein–protein and protein–solvent interactions, such as electrostatic screening and entropic interactions, also modulate protein assembly at solid–liquid interfaces.

4. Peptoids

In contrast to proteins and peptides, sequence-defined peptoids can be synthesized cheaply and efficiently using a solid-phase "submonomer" synthesis method[64] and abundant sources of primary amines that are commercially available or easy to synthesize can be used as monomers to build broad side-chain diversity.[14,64,65]

Peptoids are biocompatible and exhibit protein-like specificity and molecular recognition for biological applications,[66] while offering much higher thermal and chemical stabilities than proteins and peptides. Due to the lack of backbone hydrogen bond donors, peptoids offer unique advantages for understanding and controlling hierarchical self-assembly at solid–liquid interfaces, because tuning of peptoid–peptoid and peptoid-surface interactions can be simply achieved through the variation of side-chain chemistry.[18–20] Furthermore, these structural features of peptoids enable the introduction of a wide range of functional groups as side-chains while retaining consistent self-assembly behavior to form similar hierarchical structures.[18,21,22] Recently, directed self-assembly of sequence-defined peptoids into ordered structures on substrates with predesigned functional side-chains to match the lattice of the surfaces has received particular attention,[18,19] due to its great potential in surface coatings for biomedical applications.[67]

In a recent study, Chen et al. reported the mica-templated self-assembly of 12-mer peptoids into hexagonally patterned nanoribbons by manipulating the peptoid–peptoid and peptoid–mica interactions.[18] The 12-mer peptoid Pep-1 (**Figure 3**a) was designed to have alternating polar *N*-(2-carboxyethyl)glycines (Nce) and nonpolar *N*-[2-(4-chlorophenyl)ethyl]glycines

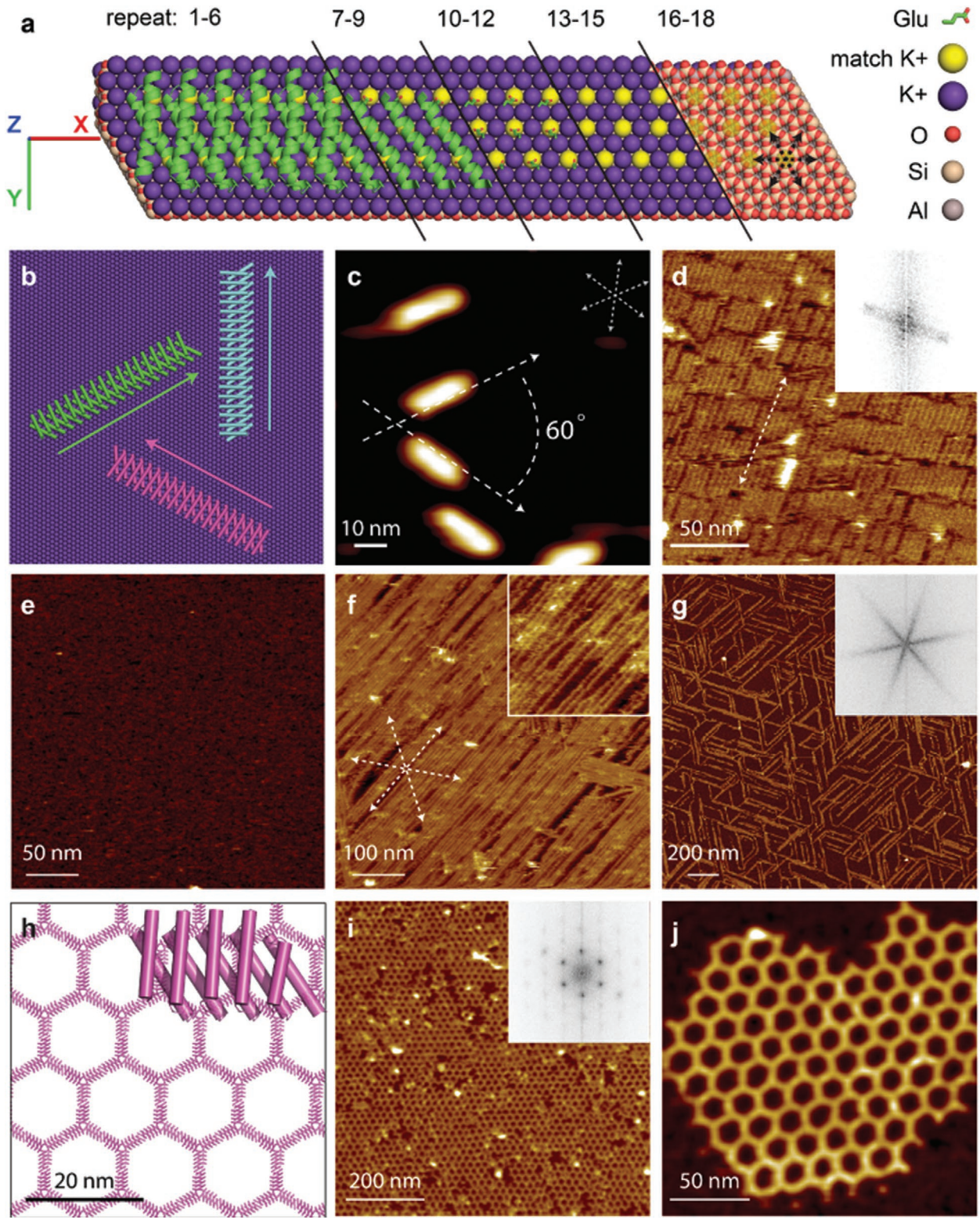

Figure 2. Designed protein interface giving epitaxial self-assembly on mica (001). a,b) Model of DHR10-mica18 matched to *m*-mica (001) via glutamate interactions with the K^+ sublattice in three symmetry-equivalent orientations. c,d) AFM images of DHR10-mica18 on *m*-mica (001) at 10×10^{-3} M and 3 M KCl, respectively. e) AFM image of DHR10-mica6 on *m*-mica (001) at 3 M KCl. f,g) AFM images of DHR10-mica6-NC self-assembled on *m*-mica (001) and *f*-mica (001), respectively, at 3 M KCl. h) Computational model of DHR10-mica5-*X*. Inset is one monomer with five repeat units. i,j) AFM images of DHR10-mica5-*X* on *m*-mica (001) at 3 M KCl at different magnifications. The insets to (d), (f), and (i) are fast Fourier transforms (FFTs). a,c–h,j) Reproduced with permission.[62] Copyright 2019, Springer Nature. b,i) Adapted with permission.[62] Copyright 2019, Springer Nature.

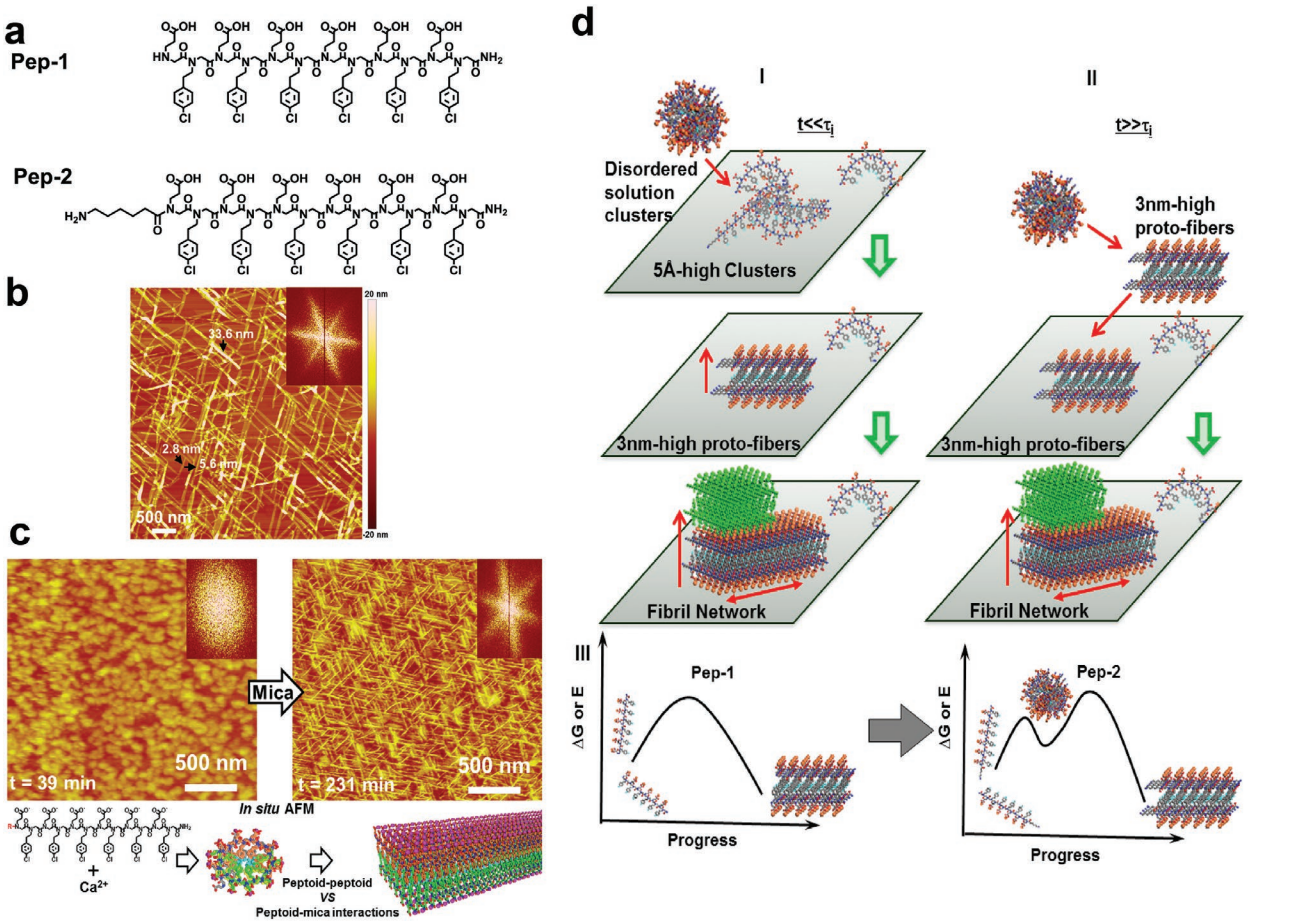

Figure 3. Surface-directed self-assembly of sequence-defined peptoids into hierarchical structures. a) Chemical structures of Pep-1 and Pep-2. b) Ex situ AFM image showing the mica-directed assembly of Pep-1 into hexagonally patterned nanoribbons; the Fourier transform (inset) shows the threefold symmetry. c) In situ AFM images of Pep-1- Ca^{2+} complexes on a mica surface showing the transformation from amorphous particles into hexagonally patterned nanoribbons at early times; the bottom is the scheme illustrating the transformation process driven by the competition between peptoid–peptoid and peptoid–mica interactions. d) Proposed assembly processes for Pep-2 at early (d-I) and late (d-II) stages and observed crystallization pathways and corresponding energy landscapes for Pep-1 and Pep-2, respectively (d-III). b,c) Reproduced with permission.[18] Copyright 2016, American Chemical Society. d) Reproduced with permission.[19] Copyright 2017, Springer Nature.

($N_{4\text{-Cl}}$pe) groups, in which Nce was used to mimic glutamic acid that enables Ca^{2+}–carboxylate interactions[68] and the aromatic $N_{4\text{-Cl}}$pe side chain was chosen because 4-chloro-substituted aromatics are known to build strong hydrophobic interactions (e.g., π–π interactions)[69] to stabilize the self-assembled structures. At pH 8.0, this peptoid self-assembled into well-aligned nanoribbons with hexagonally symmetric patterns on the mica surface in $CaCl_2$ solution (Figure 3b). The coordination of Ca^{2+}–carboxylate and bilayer-like packing of the peptoids in which interpeptoid hydrophobic interactions are built by six $N_{4\text{-Cl}}$pe side-chain groups, contributes significantly to the stability of the nanoribbons. In situ AFM studies showed that at high $CaCl_2$ concentrations ($\approx 50 \times 10^{-3}$ M) these hexagonally patterned nanoribbons were formed through an interesting particle transformation process (Figure 3c).[18] Peptoid–Ca^{2+} complexes first appeared on the mica surface as discrete nanoparticles, then gradually transformed into well-aligned nanoribbons with sixfold symmetry. Because the transformation only happened on the mica surface and AFM-based dynamic force spectrometry results confirmed that peptoid–mica interactions were much stronger than peptoid–peptoid interactions in the presence of Ca^{2+}, the authors concluded that Ca^{2+} cations located at mica-liquid interface were able to coordinate with deprotonated peptoid carboxylate groups to form multiple coordination bonds that drove the transformation of peptoid–Ca^{2+} complex particles into hexagonally patterned nanoribbons. If the concentration of Ca^{2+} was decreased to 10×10^{-3} M, no discrete particles formed before Pep-1 directly crystallized on mica. Hence, the Ca^{2+}-mediated coordination bonds formed between mica and peptoid, and between peptoid and peptoid controlled the peptoid assembly along with the interpeptoid hydrophobic interactions.

In addition to electrolytes, the attachment of headgroups, including hydrophobic, hydrophilic, and bulky subunits like cyclodextrin, to peptoid sequences can also modify self-assembly pathways and resulting structures. In a recent study by Ma et al.,[19] where a short hydrophobic region was conjugated to the above self-assembling peptoid Pep-1, the resulting peptoid Pep-2 (Figure 3a) self-assembled into a similar nanoribbon network while exhibiting a distinct crystallization pathway. With 10×10^{-3} M [Ca^{2+}], instead of directly forming crystalline

structures with Pep-1, the crystallization of Pep-2 followed a two-step pathway that began with the creation of disordered clusters of 10–20 molecules and was characterized by highly nonlinear crystallization kinetics in which clusters transform into ordered structures that then enter the growth phase (Figure 3d). Specifically, Pep-2 crystallization started with the creation of 5 Å high clusters, then the prenucleation clusters transformed into crystalline nuclei with a height of 3 nm, before extending laterally and vertically to form the 3D hexagonal network of ribbons. However, such clusters were not observed in the crystallization of Pep-1. Precise modification of self-assembling peptoids with another hydrophobic tail or a hydrophilic tail for similar self-assembly studies further confirmed that the hydrophobicity of the conjugated tail contributed to the creation of disordered precursor clusters.

Two-step nucleation pathways in which disordered, amorphous, or dense liquid states precede the appearance of crystalline phases have been reported for a wide range of materials,[50,70] but the dynamics of such pathways are poorly understood. Moreover, whether these pathways are general features of crystallizing systems or a consequence of system-specific structural details that select for direct versus two-step processes was unknown. This study made clear that system-specific structural details determine which pathway is followed. The results shed new light on nonclassical crystallization mechanisms and have implications for the design of self-assembling polymers.[19]

Inspired by cell membranes in nature, Jin et al.[22] designed and synthesized another lipid-like peptoid sequence (Pep-3). The amphiphilic peptoid, containing two blocks: six polar Nce and six nonpolar $N_{4\text{-Cl}}$pe residues (**Figure 4**a), self-assemble into a class of highly stable and self-repairable 2D membranes both in solution and on mica surfaces.[22,71] The hydrophobic interactions among $N_{4\text{-Cl}}$pe residues determined the high stability of the nanomembranes and their self-repairing and nanoscale patterning features. AFM data showed that Pep-3 self-assembled into membranes, which exhibited a thickness in the range of 3.5-4 nm and possessed very straight edges along the *x*-direction (Figure 4b). The 4.5 Å and 1.8 nm backbone-to-backbone distances along the *x*-, *y*-directions were observed by high-resolution TEM (Figure 4c) for a similar sequence (Pep-3-SH, in Figure 4a), which led to the proposed structural model for Pep-3 membranes (Figure 4d). Pep-3 exhibits anisotropic packing with stronger interpeptoid interactions along the *x*-direction than along the *y*-direction, corresponding to a faster formation rate along the *x*-direction. However, interpeptoid interactions along both directions are strong enough for peptoids to build 2D membranes.

Based on the interesting feature of β-cyclodextrin (CD) and the easy synthesis of peptoids, Jiao et al. appended this bulky CD group onto the hydrophilic Nce domain of Pep-3 to make Pep-3-CD (Figure 4a).[20] The attachment of CD to the diblock Pep-3 completely changed the self-assembly process and outcome.[20] AFM results showed Pep-3-CD initially formed 1D cylindrical micelles, and then further assembled into higher-order 2D membranes and 3D intertwined ribbons. The final morphology of peptoid assembly depended on both the substrate chemistry and the solution conditions (Figure 4e).

In situ AFM results showed that self-assembly of Pep-3-CD on SiO_2 surfaces exhibited a multistep process, forming initial spheroidal precursors before transforming into cylindrical micelles (Figure 4f). Compared to the assembly of Pep-3-CD on SiO_2, the assembly process on mica surfaces was dramatically different. Under acidic conditions ($2.1 \leq pH \leq 4.3$), Pep-3-CD first formed worm-like micelles with random orientations. These short micelles then continued to grow and ultimately covered the mica surface completely to form a continuous 2D film. Unlike the cylindrical micelles forming on SiO_2, the thickness of 2D film on mica was 4.5 nm, which was analogous with the membranes assembled from Pep-3.[22,71] However, Ca^{2+} ions could serve as bridges through Ca^{2+}–carboxylate and Ca^{2+}–CD interactions[72] to further drive the assembly of Pep-3-CD to ultimately form 3D intertwined ribbons (Figure 4g).

This study[20] revealed the self-assembly of Pep-3-CD into cylindrical micelles, 2D films, and 3D intertwined ribbons and provided insights into mechanisms and kinetics of Pep-3-CD self-assembly. To further exploit the emergent functions made possible by hierarchical self-assembly of Pep-3-CD for applications, hydrophobic 4-(2-hydroxyethylamino)-7-nitro-2,1,3-benzoxadiazole (NBD) donors were encapsulated inside the hydrophobic core, followed by exposure to Rhodamine B as acceptors that inserted into CD cages. Fluorescence emission spectra results showed that the Pep-3-CD cylindrical micelles exhibited highly efficient fluorescence resonance energy transfer in aqueous solution, mimicking natural light-harvesting systems.[20]

5. Summary and Outlook

We have summarized recent achievements in engineering the self-assembly of peptide, protein, and peptoid structures at solid–liquid interfaces. By programming biomolecular interfaces to specifically recognize certain inorganic surfaces, such as mica (001) and MoS_2 (001), controllable assembly of a range of hierarchical architectures was achieved. Moreover, the knowledge of biomolecular self-assembly and crystallization at solid–liquid interfaces from both the thermodynamic and kinetic perspectives have been enriched by using in situ AFM to monitor and study the assembly processes. The results show that numerous factors play a role in determining both the pathways and the final outcomes of assembly. In many cases, disordered precursors were found to form prior to the ordered structures, but whether such two-step pathways occur was shown to depend upon the details of primary sequence and surface interactions. Also, although designing biomolecular interfaces that create a match to the substrate chemistry and lattice structure make it feasible to assemble biomolecules into predefined architectures, other factors external to the interface design can strongly alter both the dynamics and, ultimately, the outcome of assembly. In particular, modulation of noncovalent interactions, such as hydrophobic, electrostatic and entropic interactions, between the molecules or the molecules and the substrate via solvent conditions (i.e., pH, electrolyte type and concentration, etc.), is an effective means of achieving such control. In many cases, balancing several of these noncovalent interactions is necessary to trigger self-assembly or achieve a high degree of order.

With further development and understanding, engineering of biomolecular assembly at solid–liquid interfaces to achieve

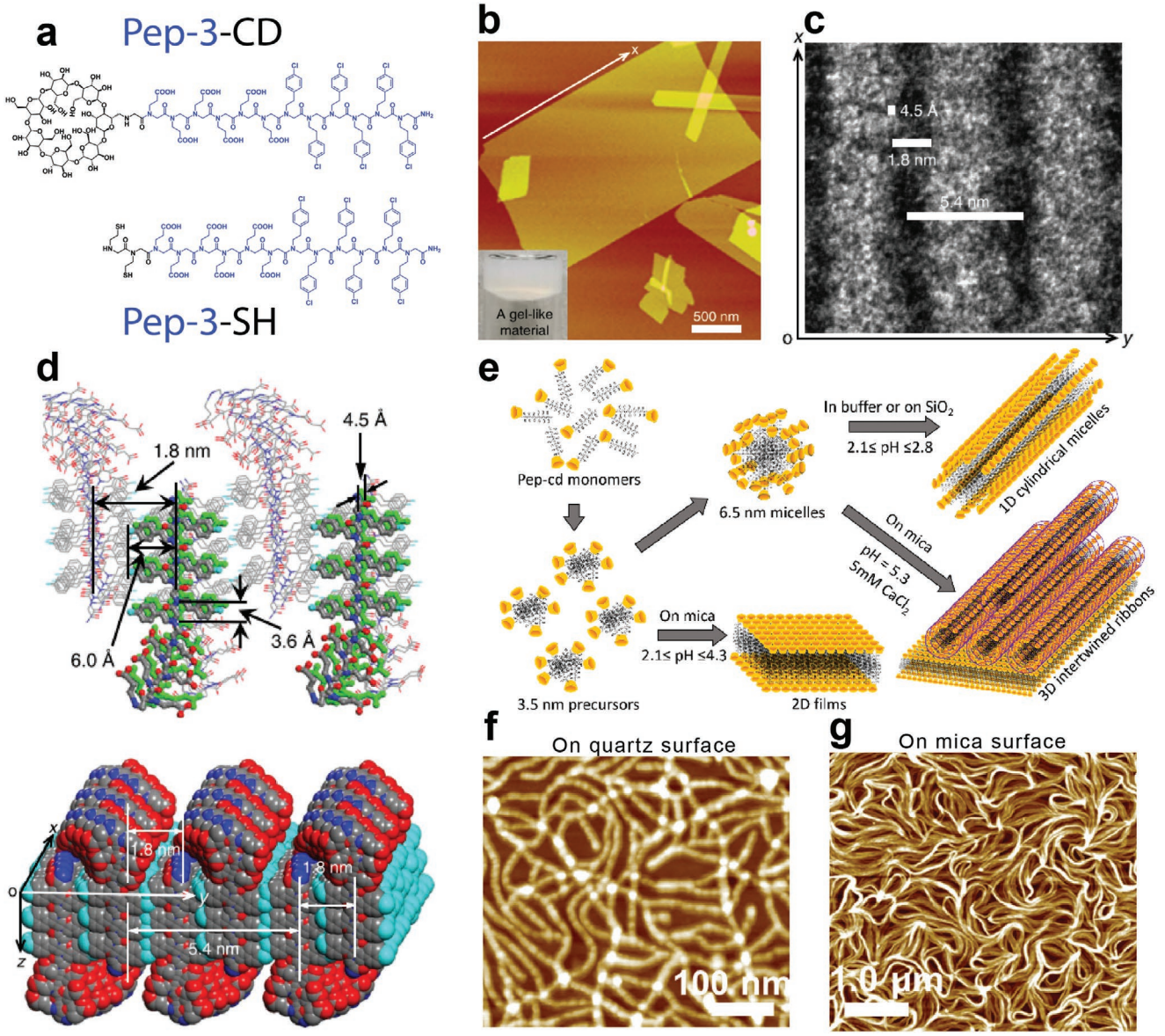

Figure 4. Surface-directed self-assembly of sequence-defined peptoids into hierarchical structures. a) Chemical structures of Pep-3 (highlighted in blue) as well as its conjugation with either a cyclodextrin (CD) group or sulfhydryl (SH) groups. b) AFM image showing Pep-3 assembled into 2D nanomembranes. c) High-resolution TEM image showing well-aligned single peptoid-wide strips in the membrane structures (Pep-3-SH[22]). d) Proposed structural model of Pep-3 membrane showing the peptoid backbone to backbone distance of 4.5 Å along the *x*-direction and 1.8 nm along the *y*-direction. e) Illustration of the assembly of Pep-3-CD into cylindrical micelles, 2D films, and 3D intertwined ribbons. f,g) AFM images showing Pep-3-CD self-assembled into 1D cylindrical micelles on quartz (pH 2.6) and 3D intertwined ribbons on mica (pH 5.3), respectively. b–d) Reproduced under the terms of the CC-BY Creative Commons Attribution 4.0 International License (http://creativecommons.org/licenses/by/4.0/).[22] Copyright 2016, The Authors, published by Springer Nature. e–g) Reproduced with permission.[20] Copyright 2019, Wiley-VCH.

precise control over diverse biomolecular and hybrid materials may enable their applications in wide range of areas, including tissue engineering, biosensing, imaging, drug delivery, diagnosis, catalysis, biomineralization, nanofabrication, electronic nanodevices, energy storage and harvesting, and environmental remediation. However, despite the impressive progress made to date, further efforts are still required to reach the stage where precise engineering of biomolecules to interface with any given solid surface and deterministically assemble into hierarchical structures is feasible. We still know little about how to control the interplay of intermolecular interactions—mainly noncovalent—and define the energy landscapes across which hierarchy develops. Furthermore, it is still difficult to predict intermediate states of self-assembly that will emerge prior to the final ordered state. Additionally, it is still challenging to design systems with multiwell potentials for out-of-equilibrium switching in response to external stimuli. Last, examples in numerous reports have proven that surfaces can alternate the assembly

kinetics and direct biomolecules toward a preferred, ordered state. We speculate that the altered hydration structure and electrolyte distribution near the solid–liquid interface is crucial in providing this guidance. However, in situ experimental capabilities for analyzing these nm-scale regions above the surface with the required Ångstrom-level precision and simulation capabilities to predict assembly over sufficiently long time and length scales are still under development. A full understanding of the thermodynamic and kinetic controls over biomolecular assembly at solid–liquid interfaces must await those developments.

Acknowledgements

S.Z., J.C., and J.L. contributed equally to this work. The work was carried out at Pacific Northwest National Laboratory (PNNL) and the University of Washington (UW) with support from the US Department of Energy, the office of Basic Energy Sciences, Energy Frontier Research Center CSSAS (The Center for the Science of Synthesis Across Scales) located at the UW (award number DE-SC0019288). PNNL is a multiprogram national laboratory operated for the DOE by Battelle under contract number DE-AC05-76RL01830.

Conflict of Interest

The authors declare no conflict of interest.

Keywords

biomolecular self-assembly, peptides, peptoids, proteins, solid–liquid interfaces

Received: September 5, 2019
Revised: April 2, 2020
Published online: July 6, 2020

[1] M. Eder, S. Amini, P. Fratzl, *Science* **2018**, *362*, 543.
[2] J. A. Marsh, S. A. Teichmann, *Annu. Rev. Biochem.* **2015**, *84*, 551.
[3] Q. Luo, C. Hou, Y. Bai, R. Wang, J. Liu, *Chem. Rev.* **2016**, *116*, 13571.
[4] G. M. Whitesides, B. Grzybowski, *Science* **2002**, *295*, 2418.
[5] K. Kinbara, T. Aida, *Chem. Rev.* **2005**, *105*, 1377.
[6] A. V. Pinheiro, D. Han, W. M. Shih, H. Yan, *Nat. Nanotechnol.* **2011**, *6*, 763.
[7] N. C. Seeman, H. F. Sleiman, *Nat. Rev. Mater.* **2018**, *3*, 17068.
[8] G. Wei, Z. Su, N. P. Reynolds, P. Arosio, I. W. Hamley, E. Gazit, R. Mezzenga, *Chem. Soc. Rev.* **2017**, *46*, 4661.
[9] S. M. Chin, C. V. Synatschke, S. Liu, R. J. Nap, N. A. Sather, Q. Wang, Z. Álvarez, A. N. Edelbrock, T. Fyrner, L. C. Palmer, I. Szleifer, M. Olvera de la Cruz, S. I. Stupp, *Nat. Commun.* **2018**, *9*, 2395.
[10] L. A. Churchfield, F. A. Tezcan, *Acc. Chem. Res.* **2019**, *52*, 345.
[11] Y. Suzuki, G. Cardone, D. Restrepo, P. D. Zavattieri, T. S. Baker, F. A. Tezcan, *Nature* **2016**, *533*, 369.
[12] P. S. Huang, S. E. Boyken, D. Baker, *Nature* **2016**, *537*, 320.
[13] H. Shen, J. A. Fallas, E. Lynch, W. Sheffler, B. Parry, N. Jannetty, J. Decarreau, M. Wagenbach, J. J. Vicente, J. Chen, L. Wang, Q. Dowling, G. Oberdorfer, L. Stewart, L. Wordeman, J. J. De Yoreo, C. Jacobs-Wagner, J. Kollman, D. Baker, *Science* **2018**, *362*, 705.
[14] J. Sun, R. N. Zuckermann, *ACS Nano* **2013**, *7*, 4715.
[15] E. J. Robertson, A. Battigelli, C. Proulx, R. V. Mannige, T. K. Haxton, L. S. Yun, S. Whitelam, R. N. Zuckermann, *Acc. Chem. Res.* **2016**, *49*, 379.
[16] Z. K. Shi, Y. H. Wei, C. H. Zhu, J. Sun, Z. B. Li, *Macromolecules* **2018**, *51*, 6344.
[17] G. L. Sternhagen, S. Gupta, Y. H. Zhang, V. John, G. J. Schneider, D. H. Zhang, *J. Am. Chem. Soc.* **2018**, *140*, 4100.
[18] C. L. Chen, R. N. Zuckermann, J. J. DeYoreo, *ACS Nano* **2016**, *10*, 5314.
[19] X. Ma, S. Zhang, F. Jiao, C. J. Newcomb, Y. Zhang, A. Prakash, Z. Liao, M. D. Baer, C. J. Mundy, J. Pfaendtner, A. Noy, C. L. Chen, J. J. De Yoreo, *Nat. Mater.* **2017**, *16*, 767.
[20] F. Jiao, X. Wu, T. Jian, S. Zhang, H. Jin, P. He, C. L. Chen, J. J. De Yoreo, *Angew. Chem., Int. Ed.* **2019**, *58*, 12223.
[21] H. Jin, Y. H. Ding, M. Wang, Y. Song, Z. Liao, C. J. Newcomb, X. Wu, X. Q. Tang, Z. Li, Y. Lin, F. Yan, T. Jian, P. Mu, C. L. Chen, *Nat. Commun.* **2018**, *9*, 270.
[22] H. Jin, F. Jiao, M. D. Daily, Y. Chen, F. Yan, Y. H. Ding, X. Zhang, E. J. Robertson, M. D. Baer, C. L. Chen, *Nat. Commun.* **2016**, *7*, 12252.
[23] L. Wang, C. Gong, X. Yuan, G. Wei, *Nanomaterials* **2019**, *9*, 285.
[24] C. Gong, S. Sun, Y. Zhang, L. Sun, Z. Su, A. Wu, G. Wei, *Nanoscale* **2019**, *11*, 4147.
[25] X. Zhang, C. Gong, O. U. Akakuru, Z. Su, A. Wu, G. Wei, *Chem. Soc. Rev.* **2019**, *48*, 5564.
[26] W. Zhang, X. Yu, Y. Li, Z. Su, K. D. Jandt, G. Wei, *Prog. Polym. Sci.* **2018**, *80*, 94.
[27] P. L. Davies, *Trends Biochem. Sci.* **2014**, *39*, 548.
[28] S. Weiner, P. M. Dove, *Rev. Mineral. Geochem.* **2003**, *54*, 1.
[29] G. Grigoryan, Y. H. Kim, R. Acharya, K. Axelrod, R. M. Jain, L. Willis, M. Drndic, J. M. Kikkawa, W. F. DeGrado, *Science* **2011**, *332*, 1071.
[30] D. L. Masica, S. B. Schrier, E. A. Specht, J. J. Gray, *J. Am. Chem. Soc.* **2010**, *132*, 12252.
[31] W. W. Leow, W. Hwang, *Langmuir* **2011**, *27*, 10907.
[32] D. M. Czajkowsky, L. Li, J. Sun, J. Hu, Z. Shao, *ACS Nano* **2012**, *6*, 190.
[33] D. Moll, C. Huber, B. Schlegel, D. Pum, U. B. Sleytr, M. Sára, *Proc. Natl. Acad. Sci. USA* **2002**, *99*, 14646.
[34] S. H. Shin, S. Chung, B. Sanii, L. R. Comolli, C. R. Bertozzi, J. J. De Yoreo, *Proc. Natl. Acad. Sci. USA* **2012**, *109*, 12968.
[35] M. Sleutel, J. Lutsko, A. E. S. Van Driessche, M. A. Durán-Olivencia, D. Maes, *Nat. Commun.* **2014**, *5*, 5598.
[36] Y. F. Dufrêne, T. Ando, R. Garcia, D. Alsteens, D. Martinez-Martin, A. Engel, C. Gerber, D. J. Müller, *Nat. Nanotechnol.* **2017**, *12*, 295.
[37] T. Ando, T. Uchihashi, S. Scheuring, *Chem. Rev.* **2014**, *114*, 3120.
[38] S. Park, K. Hamad-Schifferli, *Curr. Opin. Chem. Biol.* **2010**, *14*, 616.
[39] M. Sarikaya, C. Tamerler, A. K. Y. Jen, K. Schulten, F. Baneyx, *Nat. Mater.* **2003**, *2*, 577.
[40] S. Dogan, H. Fong, D. T. Yucesoy, T. Cousin, C. Gresswell, S. Dag, G. Huang, M. Sarikaya, *ACS Biomater. Sci. Eng.* **2018**, *4*, 1788.
[41] Y. Li, G. P. Whyburn, Y. Huang, *J. Am. Chem. Soc.* **2009**, *131*, 15998.
[42] E. Zhu, S. Wang, X. Yan, M. Sobani, L. Ruan, C. Wang, Y. Liu, X. Duan, H. Heinz, Y. Huang, *J. Am. Chem. Soc.* **2019**, *141*, 1498.
[43] C. Y. Chiu, Y. Li, Y. Huang, *Nanoscale* **2010**, *2*, 927.
[44] C. Y. Chiu, Y. Li, L. Ruan, X. Ye, C. B. Murray, Y. Huang, *Nat. Chem.* **2011**, *3*, 393.
[45] P. Li, K. Sakuma, S. Tsuchiya, L. Sun, Y. Hayamizu, *ACS Appl. Mater. Interfaces* **2019**, *11*, 20670.
[46] T. D. Jorgenson, M. Milligan, M. Sarikaya, R. M. Overney, *Soft Matter* **2019**, *15*, 7360.
[47] C. R. So, Y. Hayamizu, H. Yazici, C. Gresswell, D. Khatayevich, C. Tamerler, M. Sarikaya, *ACS Nano* **2012**, *6*, 1648.
[48] Y. Hayamizu, C. R. So, S. Dag, T. S. Page, D. Starkebaum, M. Sarikaya, *Sci. Rep.* **2016**, *6*, 33778.

[49] L. Hong, T. Nishihara, Y. Hijikata, Y. Miyauchi, K. Itami, *Sci. Rep.* **2018**, *8*, 2333.
[50] J. J. De Yoreo, P. U. P. A. Gilbert, N. A. J. M. Sommerdijk, R. L. Penn, S. Whitelam, D. Joester, H. Zhang, J. D. Rimer, A. Navrotsky, J. F. Banfield, A. F. Wallace, F. M. Michel, F. C. Meldrum, H. Cölfen, P. M. Dove, *Science* **2015**, *349*, aaa6760.
[51] J. Chen, E. Zhu, J. Liu, S. Zhang, Z. Lin, X. Duan, H. Heinz, Y. Huang, J. J. De Yoreo, *Science* **2018**, *362*, 1135.
[52] M. Nalbach, P. Raiteri, S. Klassen, S. Schäfer, J. D. Gale, R. Bechstein, A. Kühnle, *J. Phys. Chem. C* **2017**, *121*, 24144.
[53] T. C. Davis, S. R. Russell, S. A. Claridge, *Chem. Commun.* **2018**, *54*, 11709.
[54] Y. Bai, Q. Luo, J. Liu, *Chem. Soc. Rev.* **2016**, *45*, 2756.
[55] N. Hampp, *Chem. Rev.* **2000**, *100*, 1755.
[56] B. Saif, W. Zhang, X. Zhang, Q. Gu, P. Yang, *ACS Nano* **2019**, *13*, 7736.
[57] S. Gonen, F. DiMaio, T. Gonen, D. Baker, *Science* **2015**, *348*, 1365.
[58] S. Ido, H. Kimiya, K. Kobayashi, H. Kominami, K. Matsushige, H. Yamada, *Nat. Mater.* **2014**, *13*, 264.
[59] B. Stel, I. Gunkel, X. Gu, T. P. Russell, J. J. De Yoreo, M. Lingenfelder, *ACS Nano* **2019**, *13*, 4018.
[60] D. Martin-Jimenez, E. Chacon, P. Tarazona, R. Garcia, *Nat. Commun.* **2016**, *7*, 12164.
[61] T. Fukuma, Y. Ueda, S. Yoshioka, H. Asakawa, *Phys. Rev. Lett.* **2010**, *104*, 016101.
[62] H. Pyles, S. Zhang, J. J. De Yoreo, D. Baker, *Nature* **2019**, *571*, 251.
[63] M. A. Boles, M. Engel, D. V. Talapin, *Chem. Rev.* **2016**, *116*, 11220.
[64] R. N. Zuckermann, J. M. Kerr, S. B. H. Kent, W. H. Moos, *J. Am. Chem. Soc.* **1992**, *114*, 10646.
[65] A. S. Culf, R. J. Ouellette, *Molecules* **2010**, *15*, 5282.
[66] Y. Song, M. Wang, S. Li, H. Jin, X. Cai, D. Du, H. Li, C. L. Chen, Y. Lin, *Small* **2018**, *14*, 1803544.
[67] C. L. Chen, N. L. Rosi, *Angew. Chem., Int. Ed.* **2010**, *49*, 1924.
[68] R. I. Kuehnle, H. G. Boerner, *Angew. Chem., Int. Ed.* **2011**, *50*, 4499.
[69] C. L. Chen, A. M. Beatty, *J. Am. Chem. Soc.* **2008**, *130*, 17222.
[70] P. G. Vekilov, *J. Cryst. Growth* **2005**, *275*, 65.
[71] F. Jiao, Y. Chen, H. Jin, P. He, C. L. Chen, J. J. De Yoreo, *Adv. Funct. Mater.* **2016**, *26*, 8960.
[72] R. Kurapati, A. M. Raichur, *J. Mater. Chem. B* **2013**, *1*, 3175.